Structure and Optoelectronics of Electrodeposited Cadmium Ditelluride ($CdTe_2$)

Jean Rousset,*[,†,||] Pär Olsson,[†,‡] Brian McCandless,[§] and Daniel Lincot[†,||]

Institut de R&D sur l'énergie photovoltaïque, UMR 7174-EDF-CNRS-ENSCP, 6 quai Watier, 78401 Chatou Cedex, France, Laboratoire d'électrochemie et de chimie anaylytique (LECA), UMR-CNRS 7575, Ecole Nationale Supérieure de Chimie de Paris, 11 rue Pierre et Marie Curie 75231 Paris Cedex 05, France, Institute of energy conversion (IEC), University of Delaware, Newark, Delaware 19716, Département de Matériaux et Mécanique des Composants, EDF-R&D, Les Renardières, F-77250 Moret sur Loing, France

Received July 10, 2008. Revised Manuscript Received September 8, 2008

Electrodeposition is a powerful method to perform low cost, large area CdTe deposition. Good quality semiconductor materials for photovoltaic applications as well as high growth rates have been achieved using this technique. Electrodeposition in acidic solution is considered in this work. In these conditions, depending on the applied potential, a transition from the crystalline CdTe compound to a quasi-amorphous $CdTe_2$ compound has been shown. The present work explores the properties of this new compound and compares them to those of the classical electrodeposited CdTe. The experimental study (X-ray diffraction (XRD), optical transmission, and ellipsometry measurements) is complemented by theoretical results obtained by first principles modeling using density functional theory. The pyrite structure, with a lattice parameter $a = 7.250$ Å and an internal parameter $u = 0.389$, is found as the theoretically favored crystal structure. The corresponding calculated X-ray diffraction diagram is comparable to those experimentally obtained. Considering both experimental and modeling results the bandgap should be indirect with a value (1.08 eV) lower than that of electrodeposited CdTe. Moreover, this Te-rich compound is shown to be highly absorbent in the 1.5−4 eV energy range. This property can be partially explained by the flat band structure profile obtained by ab initio calculations. Finally, XRD under heating carried out on $CdTe_2$ shows that this compound is decomposed into CdTe + Te at relatively low temperature (>150 °C).

Introduction

The synthesis of CdTe has been widely studied, especially in the field of photovoltaic applications.[1−5] Indeed this binary compound presents a large band gap (1.44 eV) well suited for the solar spectrum absorption and a large absorption coefficient. Its association with a n-type CdS layer provides a good quality p−n junction. High efficiencies on small area devices (over 16% on ∼1 cm^2) and large area modules (10.5% on 0.86 m^2) have been reported.[1,2] Currently two companies (First Solar and Antec) produce CdTe-based modules with 8−9% baseline efficiencies.

Even if most studies have been focused on physical deposition methods (vacuum evaporation,[3] CSS[4,5]), electrodeposition was demonstrated as a really efficient method to perform large-scale and low cost thin film deposition. The pioneering work[6] published in 1978 demonstrated the feasibility of CdTe electrodeposition based on the underpotential deposition of Cd on a previously deposited Te monolayer. Numerous reports allowed optimization the deposition conditions (bath composition, applied potential (or current), and hydrodynamic conditions) to obtain good quality as-grown material. BP Solar achieved in 2001 the realization of electrodeposited modules with a record efficiency of 10.6% on large area 0.9 m^2.

Studies[7,8] focused on the possibility of enhancing the growth rate of the binary compound by varying the pH of the electrolyte. The use of very acidic pH (1 or 1.5) increases the solubility of the tellurium precursor in water, which is one of the limiting factors of the electrochemical method. In that case, depending on the applied potential and on the hydrodynamic conditions, the formation of a Te-rich compound, namely, $CdTe_2$, has been demonstrated. This compound appears when the potential is shifted toward less cathodic potentials than that usually applied to obtain a stoichiometric CdTe compound. Te-rich compounds have received great attention in the context of the deposition of a

* Corresponding author. E-mail: jean-externe.rousset@edf.fr. Tel: +33 1 30 87 78 45. Fax: +33 1 30 87 85 65.
† Institut de R&D sur l'énergie photovoltaïque.
|| Laboratoire d'électrochemie et de chimie anaylytique.
‡ Département de matériaux et mécaniques des composants.
§ Institute of energy conversion.

(1) Green, M.; Emery, K.; King, D.; Igari, S.; Warta, W. *Prog. Photovoltaics* **2002**, *10*, 55 (Solar cell efficiency tables: version 19).
(2) Wu, X.; Dhere, J. C.; Dehart, R. G.; Albin, C.; Duda, D. S.; Gessert, T. A.; Asher, S.; Levy, D. H.; Sheldon, P. *Proceedings of the 17th European Photovaics Solar Energy Conference*, Munich, 2001; WIP-Munich and ETA-Florence: Munich, 2002; p 995.
(3) Romeo, N.; Bosio, A.; Tedeschi, R.; Canevari, V. *Mater. Chem. Phys.* **2000**, *66*, 201.
(4) Romeo, N.; Bosio, A.; Tedeschi, R.; Canevari, V. *Thin Solid Films* **2000**, *361*, 327.
(5) Wu, X. *Sol. Energy* **2004**, *77*, 803.
(6) Panicker, M. P. R.; Knaster, M.; Kroger, F. A. *J. Electrochem. Soc.* **1978**, *125*, 566.
(7) Lepiller, C.; Lincot, D. *J. Electrochem. Soc.* **2004**, *151*, C348.
(8) Rousset, J.; Lincot, D. *J. Electrochem. Soc.* **2007**, *154*, D310.

10.1021/cm801887v CCC: $40.75
Published on Web 10/04/2008

good ohmic contact on the CdTe. Indeed this p-type material shows a high electron affinity which leads to the creation of a large Schottky barrier, decreasing the efficiency of the electron collection. To make this barrier as small as possible, Te rich compounds such as Sb_2Te_3[4] have been successively used.

In this present paper, structural and optical properties of the $CdTe_2$ compound are explored. The experimental study is complemented by theoretical results obtained by first principles modeling using density functional theory.

Experimental Section

Electrochemical Conditions. Electrodeposition was performed at 70 °C in a conventional three-electrode cell using a VMP2 potentiostat from Princeton Applied Research coupled with the Ec-laboratory software. The reference electrode was a saturated K_2SO_4 mercurous sulfate electrode (MSE, +0.65 V vs the standard hydrogen electrode), separated from the solution by an Al_2O_3 porous junction and maintained at room temperature by a glass bridge filled by the electrolyte. A Pt wire served as the counter electrode and was placed inside an open glass tube to prevent back diffusion in the solution of O_2 formed during the experiment. The working electrode was made of a cadmium sulfide thin film deposited by chemical bath deposition on a transparent conducting tin oxide coated glass plate, kindly supplied by BP Solar. For all experiments presented here the electrolytic solution was prepared by dissolving 0.2 mol/L of Cd(II) ions (the precursor salt was 3 $CdSO_4 \cdot 8H_2O$ from Alfa Aesar) in a saturated solution of TeO_2 (TeO_2, 99.995% from Aldrich). The water used was deionized and had a resistivity of 18 MΩ·cm (Millipore). The solution was deaerated by bubbling an inert gas (argon), also during all the experiments. A rotating electrode (Radiometer Analytical) was used to obtain a well defined hydrodynamic regime. The rotation rate was fixed at 200 rounds per minute (rpm). The films were electrodeposited at different potentials which describe the current plateau observed between −0.6 and −1.1 V on the $I-V$ curve.

Characterization. Morphology and composition of the films were studied by scanning electron microscope (SEM) and energy dispersive spectroscopy (EDS), respectively. The microstructure of the films was examined by XRD using the Cu Kα radiation. Optical properties of the materials were investigated by optical transmission and variable angle spectroscopic ellipsometry (VASE). To determine the optical constants of the deposited films, those of glass, SnO_2, and CdS are needed. The optical constants of SnO_2 were obtained from the database of optical constants from Anstrom Sun Technologies Inc. CdS film is considered to be the same as in previous studies.[9] For the fitting of the ellipsometry coefficients, the simple model consists of four layers and a surface roughness component using a layer model previously developed by the IEC group for CdS/SnO_2/glass structures. The quality of the experimental data (ψ and Δ) fits is indicated by the MSE factor which has to be <20.

Calculation Method. The ab initio calculations were performed in the framework of density functional theory (DFT) using a projector augmented wave representation of the wave functions as implemented in the VASP code.[10−14] The exchange-correlation was treated using the generalized gradient approximation with the parametrization by Perdew et al.[15] The cell parameters for the different crystal structures were all stepwise fully relaxed to minimize the Hellmann−Feynman forces within their respective symmetries. The Brillouin zone sampling was performed according to the method of Monkhorst and Pack[16] with a k-point density of at least 0.6 $Å^{-3}$. The plane-wave energy cutoff was chosen for all cases to be 400 eV. The total energy was thus converged with respect to k-points and energy cutoff to within 0.2 meV/atom. The electronic configurations used were for Cd, with 12 electrons explicitly in the valence, $Kr4s^24d^{10}$, and for Te, with 6 electrons explicitly in the valence, $Cd5s^25p^4$.

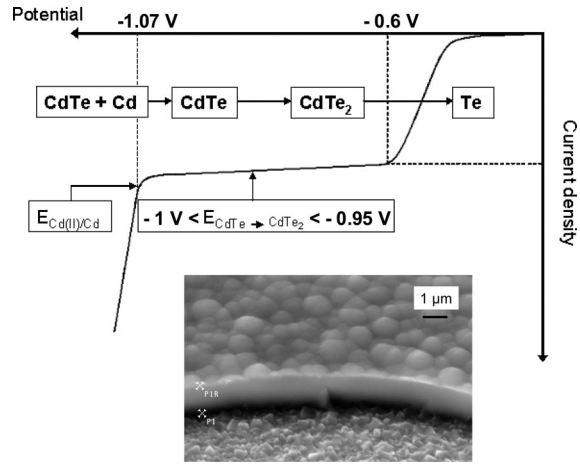

Figure 1. Schematic representation of an $I-V$ curve in the Cd(II)/Te(IV) system. Evolution of the material composition as a function of the applied potential. Morphology of a 1 μm thick $CdTe_2$ layer.

Results and Discussion

Previous studies[7,17] have shown that the composition and the optoelectronic properties of the electrodeposited material strongly depend on the applied potential. Three different potential intervals have been defined corresponding to the formation of different materials as illustrated in Figure 1. CdTe, $CdTe_2$, and pure Te phases are successively formed when the applied potential is displaced in the deposition plateau (between −0.6 V and −1.1 V). A stoichiometric compound is deposed at pH = 1.5 in a potential interval ranging from −1.1 V to −1 V; for less cathodic potentials (between −0.95 V and −0.8 V) a material presenting a large excess of tellurium with a constant Cd/Te atomic ratio of 1/2 is obtained, corresponding to the $CdTe_2$ compound.

X-ray Diffraction Study. *Room Temperature.* The XRD pattern obtained for the material electrodeposited at −1 V (which presents a composition Cd/Te close to 1/1) is presented in Figure 2a. It contains peaks characteristic of both CdTe and rutile-SnO_2 phases (marked by ▲). The SnO_2 phase is detected since the thickness of the CdTe film (≈1 μm) is lower than the X-ray penetration distance in the material. Peaks which appear at $2\theta = 23.8°$, 39.3°,and 46.4° can be respectively attributed to the diffraction of the (111), (220), and (311) planes of the CdTe cubic structure. The

(9) Paulson, P. D.; McCandless, B. E.; Birkmire, R. W. *J. Appl. Phys.* **2004**, *95*, 3010.
(10) Kresse, G.; Hafner, J. *Phys. Rev. B* **1993**, *47*, 558.
(11) Kresse, G.; Furthmüller, J. *Phys. Rev. B,* **1996**, *54*, 11169.
(12) Kresse, G.; Furthmüller, J. *Comput. Mater. Sci.* **1996**, *6*, 15.
(13) Blöchl, P. E. *Phys. Rev. B* **1994**, *50*, 17953.
(14) Kresse, G.; Joubert, D. *Phys. Rev. B* **1999**, *59*, 1758.
(15) Perdew, J. P.; Burke, K.; Ernzerhof, M. *Phys. Rev. Lett.* **1996**, *77*, 3865.
(16) Monkhorst, H. J.; Pack, J. D. *Phys. Rev. B* **1976**, *13*, 5188.
(17) Kampmann, A.; Cowache, P.; Mokili, B.; Lincot, D.; Vedel, J. *J. Cryst. Growth* **1995**, *146*, 256.

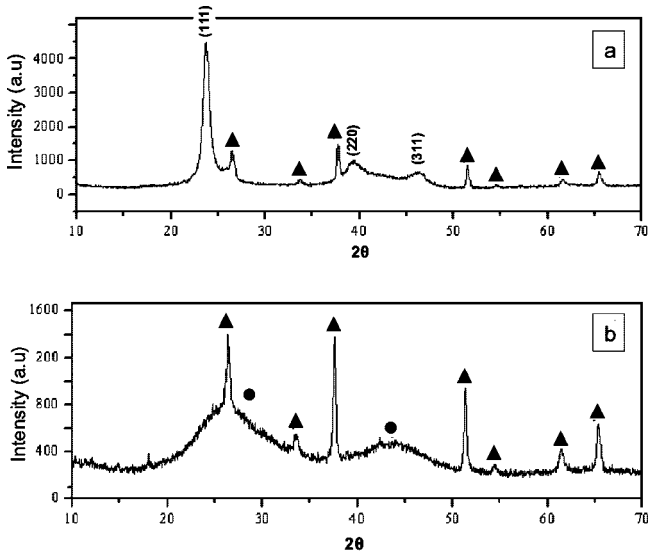

Figure 2. XRD diagrams obtained for films deposited at −1 V/SME (a) and −0.95 V/SME (b). Rutile-SnO_2 phases and $CdTe_2$ phases marked by ▲ and ●, respectively.

intensity of the (111) peak is higher than that calculated for a powder diagram due to the preferential orientation of the film along this crystallographic direction, in agreement with previous studies.[17] The crystallite size in the [111] direction has been estimated by the Scherrer relationship and is about 20 nm.

The shift of the applied potential from −1 V to −0.95 V induced a dramatic change of the X-ray pattern Figure 2b. No CdTe cubic structure peak can be observed for the sample deposited at −0.95 V, and despite a large excess of tellurium atoms (Cd/Te ≈ 1/2), no significant Te crystalline precipitates or inclusions are detected. Features present on the X-ray diagram are broad, and weak bands appear centered at $2\theta = 26.2°$ and $2\theta = 44°$ (marked by ●). Their large FWHMs show that the material is nanostructured with a crystallite size lower than 1 nm.

Proposed Crystalline Structure for $CdTe_2$. Because of the weak signal obtained during the XRD characterization and consequent difficulty in uniquely determining the crystal structure, ab initio calculations were performed on several AB_2 stoichiometric structures (Strukturbericht type C). These calculations allow the determination of the theoretical stability of the given structures and thus provide a viable candidate for $CdTe_2$. The structural assumptions, shown in Figure 3, were allowed to relax completely inside their given symmetries, thus providing predictions of the equilibrium structural parameters, such as the density of the compound and internal bond lengths.

These quantities were verified by measurements. The structures studied here were Pyrite C2 (space group $Pa\bar{3}$) and the symmetrically closely related Fluorite C1 (space group $Fm3m$: tetrahedral interstitial Te occupation of the cubic CdTe structure), Marcasite C18 (space group $Pnnm$), and the trigonal ω C6 (space group $P\bar{3}m1$). Some known compounds that have these structures are, for Pyrite, CdS_2, $CdSe_2$;[18] for Fluorite, CdF_2;[19] for Marcasite, $CaCl_2$; and for ω C6, CdI_2.[20] The ground-state energies of the relaxed

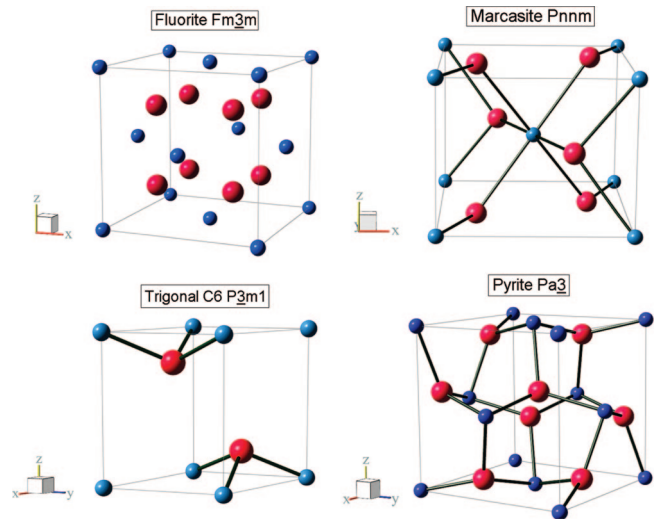

Figure 3. Representation of the different structural assumptions. Tellurium and cadmium atoms are represented by the bigger balls and the smaller balls, respectively.

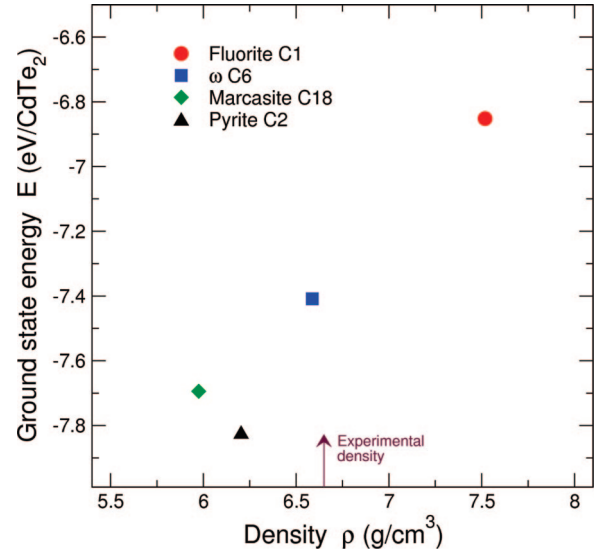

Figure 4. Densities and ground-state energies predicted ab initio. The most stable is the Pyrite C2 structure.

Table 1. Predicted Parameters of the Different Structures[a]

structure	ρ_{eq} (g/cm^3)	a (Å)	b (Å)	c (Å)	U	space group
fluorite C1	7.518	7.222				$Fm\bar{3}m$
marcasite C18	5.975	5.951	6.922	4.802	0.195, 0.390	$Pnnm$
trigonal ω C6	6.587	4.36		5.45	0.298	$P\bar{3}m1$
pyrite C2	6.204	7.250			0.389	$Pa\bar{3}$

[a] The parameter u represents the internal structure; in the case of marcasite both the x and the y internal parameters are given.

structures are presented in Figure 4 with respect to their predicted equilibrium densities. The predicted structural parameters of the different structures are shown in Table 1.

From the values in Table 1 the theoretical XRD diagrams are calculated using the freeware PowerCell 2.4. Comparison between the experimental XRD diagram and the calculated ones is presented in Figure 5 for the four proposed structures. The small size of the $CdTe_2$ crystallites causes a large increase of the peak FWHMs, which is taken into account in the XRD simulation. Thus the two experimental peaks

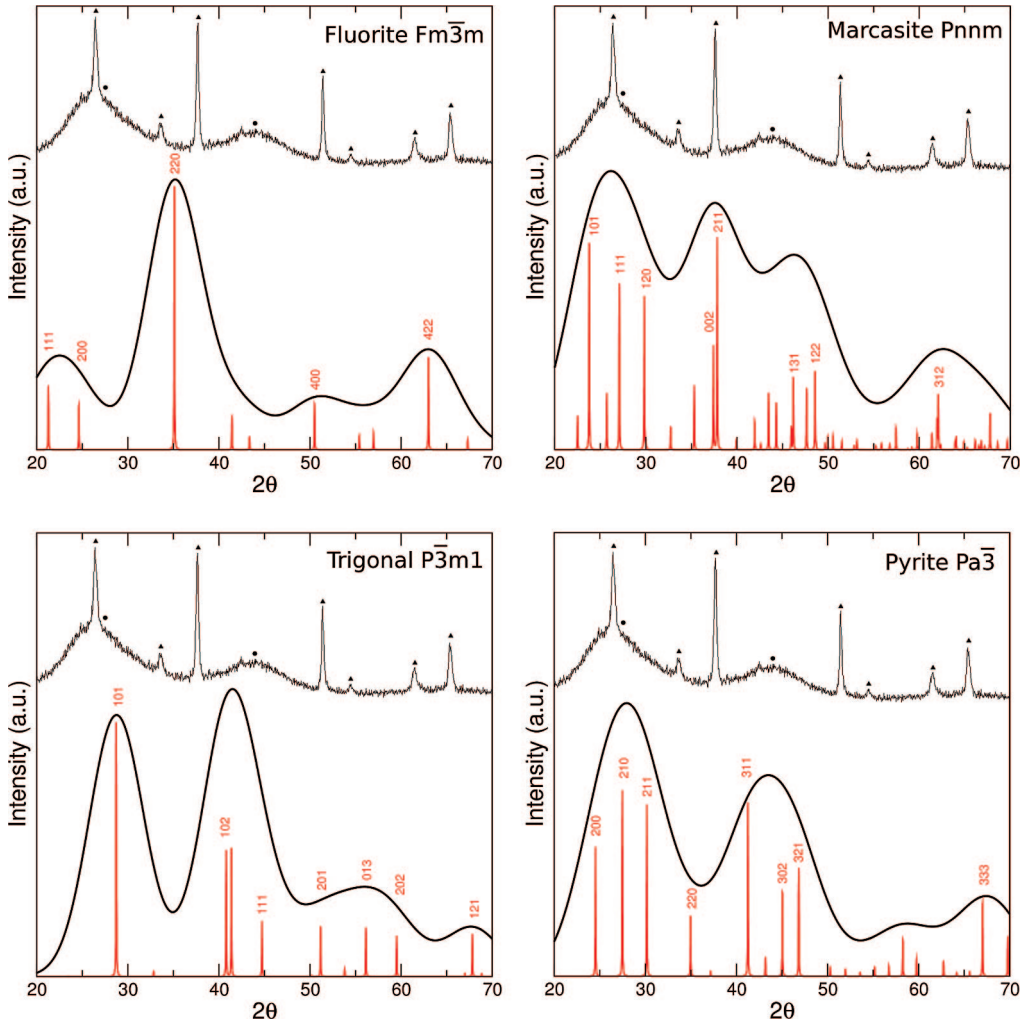

Figure 5. Comparison between the $CdTe_2$ experimental XRD diagram and the theoretical XRD diagram obtained for each structural assumption.

can be due to the overlapping of reflections of different reticular plane families.

Moreover, the experimental density of the $CdTe_2$ is evaluated from the comparison between the consumed charge during the electrodeposition and the thickness of the film. These two parameters are connected by the classic Faraday law. The global electrochemical reaction considered for this calculation is the consumption of 10 mol of electrons for the production of 1 mol of $CdTe_2$.

$$Cd^{2+} + 2HTeO_2^{+} + 10e^{-} + 6H^{+} \rightarrow CdTe_2 + 4H_2O \quad (1)$$

The density can be approximated using the two assumptions of a homogeneous compound deposition and of an electrochemical efficiency of 100%. A 7855.1 ± 4.5 Å (thickness measured by ellispsometry) thick film has been deposited consuming 1.077 C on a 1 cm^2 surface electrode corresponding to an experimental density of 6.65 $g \cdot cm^{-3}$.

As can be seen from Figure 4, the Pyrite structure is the theoretically favored crystal structure, and its equilibrium density is within the expected range with respect to the experimental one. Directly from the comparison of the densities, one cannot safely distinguish which structure corresponds to the experimental one. However, of the theoretical XRD diagrams that these structures give rise to only the Pyrite is comparable with the measured one; see Figure 5. For this structural assumption, the number of diffracting plane families is quite high. So the experimental peaks at $2\theta = 26.2°$ and $2\theta = 44°$ can be respectively considered as the responses of (200), (210), and (211) planes for the first one and of (311), (222), (302) and (312) for the second one. This result can be compared with the work of Bither et al.[18] which deals with the synthesis and characterization compounds chemically close to the $CdTe_2$, such as CdS_2 or $CdSe_2$. Those transition metal dichalcogenide crystallize in the pyrite structure with a lattice parameter that increases with the size of the anion considered (6.303 Å for the cubic structure of CdS_2, 6.615 Å for $CdSe_2$, and 7.25 Å for $CdTe_2$proposed here).

Influence of Heat Treatment. Electrodeposited CdTe films were annealed at 350, 400, and 450 °C, for 30 min in air. The annealing resulted in two effects, first the intensity of the (111) peak increased, while its fwhm decreased with the temperature, showing an improvement of the crystalline properties of the film. For the sample treated at 350 °C the

(18) Bither, T. A.; Bouchard, R. J.; Cloud, W. H.; Donohue, P. C. *Inorg. Chem.* **1968**, *7*, 2208.
(19) Deligoz, E.; Colakoglu, K.; Ciftci, Y. O. *J. Alloys. Comp.* **2007**, *438*, 66.
(20) Wykoff, R. W. G. *Crystal structures*; Interscience publishers: New York, 1963; Vol. 1.

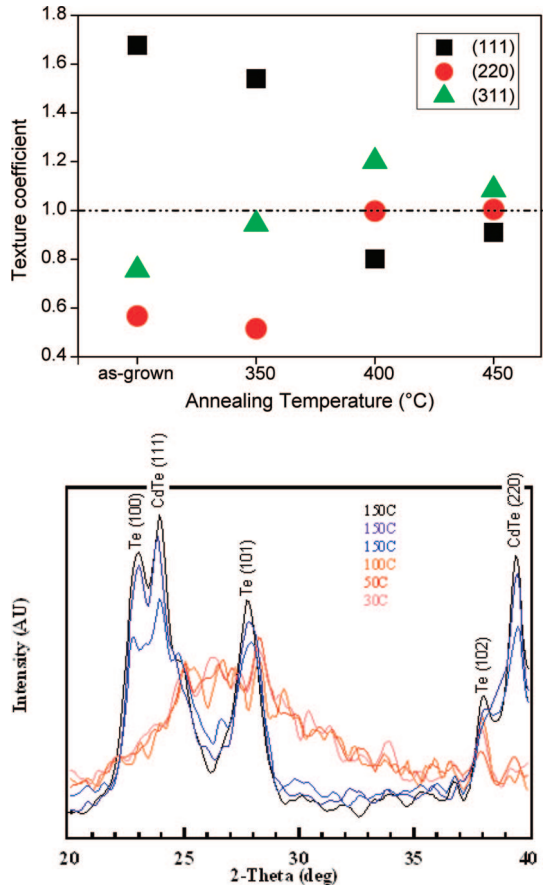

Figure 6. Top: CdTe, texture coefficient evolutions for the (111) (♦), (220) (□), and (311) (▲) crystalline directions as a function of the heat treatment temperature. Bottom: $CdTe_2$, XRD diagram evolution as a function of the heat treatment temperature.

(111) peak intensity stays much higher than the response of the (220) and (311) planes, so the preferential orientation was preserved. Inversely, an increase of temperature led to a decrease of the ratio between the intensity of the (111) peak and (220) and (311) peaks, characteristic of the recrystallization of the CdTe film. This phenomenon can be quantified considering the texture coefficients of the (111), (220), and (311) planes using the following relation:

$$C_{i(hkl)} = \frac{\frac{I_{i(hkl)}}{I_{0(hkl)}}}{\frac{1}{N}\cdot\sum_{i=1}^{N}\frac{I_{i(hkl)}}{I_{0(hkl)}}} \qquad (2)$$

where $I_{0(hkl)}$ is the standard diffraction intensity in the [*h*, *k*, *l*] direction of a random sample, $I_{(hkl)}$ the observed diffraction intensity in the [*h*, *k*, *l*] direction, and *N* the number of diffraction peaks. For a preferentially oriented sample along a [*h*, *k*, *l*] direction, the corresponding texture coefficient should be greater than one. The significant evolutions of $C_{(1,1,1)}$, $C_{(2,2,0)}$, and $C_{(3,1,1)}$ to values close to unity show the loss of the preferential orientation of the CdTe film during the annealing for temperatures greater than 350 °C (Figure 6, top). To evaluate the stability of the $CdTe_2$ compound with temperature, XRD diffraction experiments have been carried out in situ in a furnace under a He atmosphere. For temperatures below or equal to 100 °C, the XRD pattern stays similar to the one previously described for the $CdTe_2$ compound. When this material was heated to 150 °C the broad peak centered at $2\theta = 26.2°$ disappeared and was replaced by peaks at $2\theta = 23°$, 23.9°, 27.7°, 38°, 39°, and 39.4° which can be attributed to the diffraction of a mix of CdTe and Te phases (Figure 6, bottom). Consequently the $CdTe_2$ was transformed into two more stable phases at a relatively low temperature.

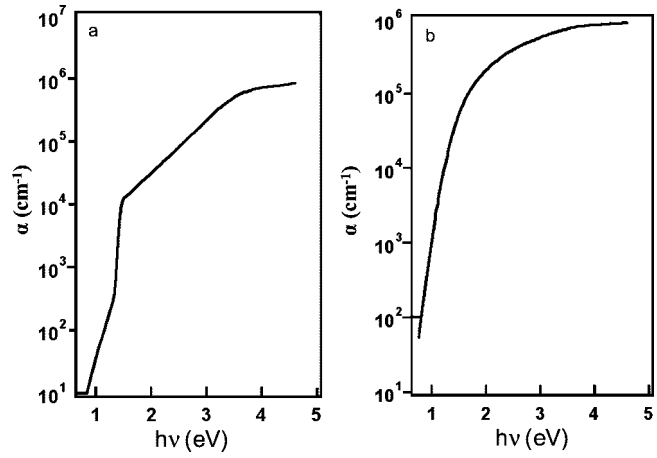

Figure 7. CdTe (a) and $CdTe_2$ (b) absorption coefficients obtained by optical transmission and ellipsometry.

Optoelectronic Properties. The evolution of the bandgap width with the applied potential, experimentally shown by the shift of the transmission onset to higher wavelength values, has been investigated by Lepiller et al.[7] The $CdTe_2$ and CdTe bandgap values determined by optical transmission experiments are respectively 1.45 eV (direct band gap; extrapolation of $(\alpha\cdot h\nu)^2$ as a function of $h\nu$) and around 1.3 eV (with the assumption of a direct bandgap) or, alternatively, for the $CdTe_2$, 1 eV (with the assumption of an indirect bandgap; extrapolation of $(\alpha\cdot h\nu)^{1/2}$ as a function of $h\nu$).

Variable angle spectroscopic ellipsometry (VASE) reflection was also carried out on as-deposited CdTe and $CdTe_2$ with incident energies ranging from 0.7 to 4.5 eV. The absorption coefficients of the films have been calculated from the experimentally determined extinction coefficients by the usual equation $\alpha = 4\pi k/\lambda$ (Figure 7). By this technique, an absorption coefficient which varied from 4×10^4 cm^{-1} to 8×10^5 cm^{-1} for the $CdTe_2$ phase and an absorption coefficient which varied from 10^4 cm^{-1} and 8×10^5 cm^{-1} for CdTe in the 1.5−4 eV energy range were obtained. In the case of the CdTe phase, the variation of $(\alpha\cdot h\nu)^2$ was linear for incident energies close to the bandgap width. This behavior, characteristic of a direct transition, allows us to determine $E_g \approx 1.44$ eV. In the case of the $CdTe_2$ phase a bandgap width of 1.08 eV was obtained by the plot of $(\alpha\cdot h\nu)^{1/2}$, which is characteristic of an indirect transition.

Due to the apparent difficulty in determining the character (direct or indirect) of the bandgap, the band structure of the Pyrite structure has been calculated ab initio; see Figure 8. The bandgap predicted by DFT of 0.42 eV is, as usual, underestimated, but the structure of the valence and conduction bands were well represented. It is seen from Figure 8 that the pyrite $CdTe_2$ has an indirect bandgap with a very flat structure. Considering both experimental and modeling

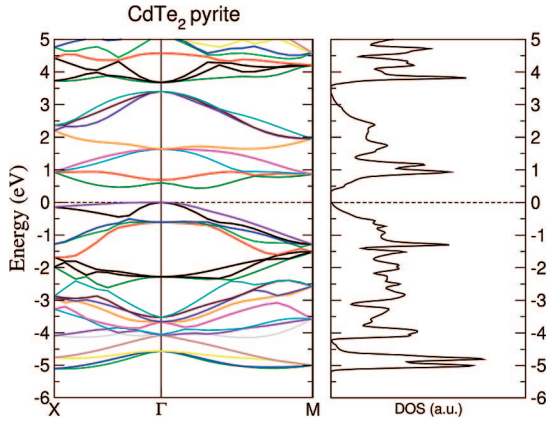

Figure 8. Left: band structure of Pyrite $CdTe_2$ from the X to Γ to M points in the reciprocal space. Right: density of states for Pyrite $CdTe_2$ in arbitrary units.

results, the bandgap of $CdTe_2$ should therefore be indirect with a value of 1.08 eV. The flatness of the bandstructure could explain the difficulty in discerning the character of the bandgap from the transmission measurements. Also the high absorption coefficient could be partly explained by this feature, as also transitions away from the zone center should have significant cross sections. The optical properties of the $CdTe_2$ compound, especially the elevated refractive index (determined by ellipsometry measurements, not shown), are consistent with the properties of chalocgenide glasses reported for other chemical systems.[21]

(21) Pandey, V.; Mehta, N.; Tripathi, S. K.; Kumar, A. *Chalcogenide Lett.* **2005**, *2*, 39.

Conclusions

The structural and optical properties of the $CdTe_2$ have been investigated and compared to those of electrodeposited CdTe. Connecting experimental and simulated XRD diagrams with theoretical calculations allowed us to propose the assumption of the pyrite structure as the more stable among those frequently encountered for AB_2 compounds. The metastable character of the $CdTe_2$ phase has been shown by in situ XRD measurements in a furnace. This compound is transformed at relatively low temperatures (between 100 and 150 °C) into a mix of CdTe and Te phases. In contrast, the electrodeposited CdTe is stable under heating and tends to recrystallize for temperatures superior to 400 °C. Optical transmission and ellipsometry experiments coupled with ab initio calculations show that the $CdTe_2$ bandgap is indirect and smaller than that of CdTe. The high absorption of this compound (observed by VASE measurements) can be tentatively explained by the very flat bandstructure obtained by DFT calculations. With a high absorption coefficient coupled with a low band gap value the $CdTe_2$ could be regarded as an interesting absorber in the visible range.

Moreover, the $CdTe_2$ compound which can be easily grown on a CdTe substrate may represent an interesting alternative as a buffer layer to create an ohmic contact between the absorber films and the metallic contact for photovoltaic applications.

Acknowledgment. We thank Dr. Charles Delacourt at Laboratoire de Réactivité et Chimie des Solides for XRD measurements and CEA/LETI for support and participation in this study.

CM801887V